Realization of the National Institute of Standards and Technology detector-based spectral irradiance scale

Howard W. Yoon, Charles E. Gibson, and Patricia Y. Barnes

A detector-based spectral irradiance scale has been realized at the National Institute of Standards and Technology (NIST). Unlike the previous NIST spectral irradiance scales, the new scale is generated with filter radiometers calibrated for absolute spectral power responsivity traceable to the NIST high-accuracy cryogenic radiometer instead of with the gold freezing-point blackbody. The calibrated filter radiometers are then used to establish the radiance temperature of a high-temperature blackbody (HTBB) operating near 3000 K. The spectral irradiance of the HTBB is then determined with knowledge of the geometric factors and is used to assign the spectral irradiances of a group of 1000-W free-electron laser lamps. The detector-based spectral irradiance scale results in the reduction of the uncertainties from the previous source-based spectral irradiance scale by at least a factor of 2 in the ultraviolet and visible wavelength regions. The new detector-based spectral irradiance scale also leads to a reduction in the uncertainties in the shortwave infrared wavelength region by at least a factor of 2–10, depending on the wavelength. Following the establishment of the spectral irradiance scale in the early 1960s, the detector-based spectral irradiance scale represents a fundamental change in the way that the NIST spectral irradiance scale is realized. © 2002 Optical Society of America

OCIS codes: 120.3930, 120.3940, 120.4800, 120.5630.

1. Introduction

The development and use of cryogenic radiometers have led the trend toward decreasing uncertainties in the radiometric and the photometric scales because of improvements in the absolute power measurements.[1,2] Furthermore, detector-based scales often can be maintained with shorter measurement chains and lower uncertainties than source-based scales. For example, the photometric scale at the National Institute of Standards and Technology (NIST) has been detector based and traceable to the NIST high-accuracy cryogenic radiometer (HACR) since 1993,[3] and the implementation of the detector-based photometric scale resulted in a factor of 2 reduction in the expanded uncertainties compared with the previous source-based photometric scale.[4] Because the radiometric quantities of spectral radiance and spectral irradiance require measurements at many different wavelengths compared with the single measurement in the assignment of a photometric quantity, the establishment of a detector-based spectroradiometric scale has proven more time-consuming.

The spectral radiance and the radiance temperature scale at NIST have all been based on the absolute radiometric determination of the freezing temperature of gold,[5] and the spectral irradiance scale is in turn realized from the spectral radiance scale.[6] As shown in Fig. 1(a), during the process of scale realization, the radiance temperature at 655 nm is assigned to a vacuum tungsten-filament lamp (gold-point lamp) operated to match the radiance temperature of the gold freezing-temperature blackbody. The radiance temperature of a tungsten lamp operated at a higher temperature (1530 K) is in turn determined with the gold-point lamp, and the radiance temperature of a variable-temperature blackbody (VTBB) is assigned. The VTBB has a small 2-mm-diameter opening, and the estimated emissivity of the VTBB is 0.9990 ± 0.0005 based on the geometry and temperature uniformity.[7] The spectral radiance of tungsten-filament lamps and integrating sphere sources is assigned by use of the

The authors are with the Division of Optical Technology, National Institute of Standards and Technology, Mail Stop 8441, Gaithersburg, Maryland 20899. H. W. Yoon's e-mail address is hyoon@nist.gov.

Received 7 January 2002; revised manuscript received 6 June 2002.

0003-6935/02/285879-12$15.00/0

© 2002 Optical Society of America

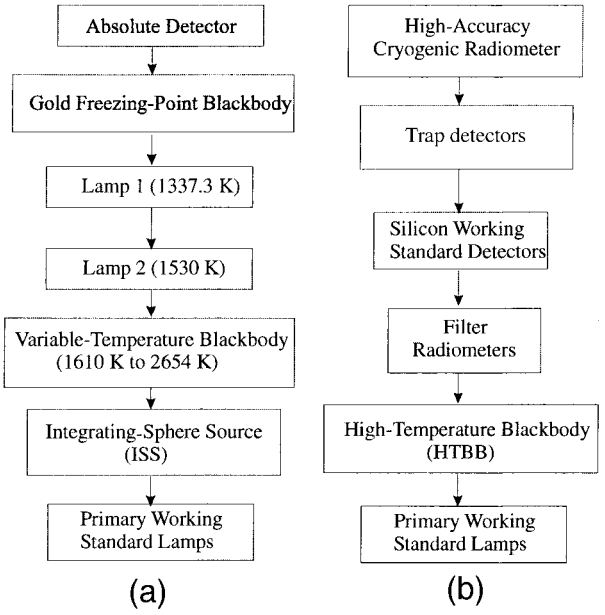

Fig. 1. (a) Measurement chain used to derive the source-based spectral irradiance scale used in the 1990 and 1992 scale realizations. (b) The measurement chain used in the new detector-based spectral irradiance scale of 2000.

VTBB; and typically, the temperature of the VTBB is changed to match the spectral radiance of the sources to minimize the effects that are due to the nonlinear responsivities of the detectors. For spectral irradiance realizations, the spectral radiance of an integrating-sphere source (ISS) is assigned, and the ISS is fitted with a precision aperture for use as a source of known spectral irradiance to calibrate a set of 1000-W free-electron laser (FEL) lamps.

The source-based spectral irradiance scale realization procedure is long and involves many separate steps to assign the spectral irradiance of a set of lamps. The primary reason for the long calibration chain is the low spectral radiance output of the gold freezing temperature blackbody at 1337.33 K.[8] Because the 1000-W FEL lamps have spectral shapes similar to that of a 3000 K blackbody, the radiant output of the intermediate transfer artifacts must be progressively increased to eventually match the spectral irradiance output of the 1000-W FEL lamp. Furthermore, a major contribution to the final uncertainties in the spectral irradiance scale is due to the temporal drift of the ISS and the low signal of the ISS, especially in the shortwave infrared region. The temporal drift of the ISS also depended on the wavelength region, resulting in greater temporal changes in the ultraviolet wavelength region. The spectral irradiance scale was difficult to realize at many different wavelengths because of a possible temporal drift resulting from the additional time needed for realizations.

In the past decade, new developments in the construction of high-temperature blackbodies (HTBBs) made from pyrolytic graphite have allowed prolonged (>100 h) operations at or above 3000 K.[9] Furthermore, at NIST the uncertainties in the detector power responsivity scale were reduced with the advent of the HACR as the primary standard for spectral power responsivity calibrations. The advantages of the new detector-based scale realization are evident in Fig. 1(b), with a much shorter chain from the cryogenic radiometer to the primary working standards compared with the measurement chain shown in Fig. 1(a). In the realization of the detector-based scale, the filter radiometers (FRs) are used to determine the temperature of the HTBB, and then the spectral irradiance output of the HTBB is used to directly calibrate the primary working standard lamps.

In this paper we describe the realization of the NIST detector-based spectral irradiance scale. The FRs used to determine the radiance temperature of the HTBB are characterized, and the agreement between the absolute detector-based radiance temperatures are compared with those found by use of the International Temperature Scale of 1990 (ITS-90).[10] The agreement between the detector-based and the gold freezing-temperature-based spectral radiances is also shown to verify that the HTBB spectral radiance does not deviate significantly from a single-temperature Planck radiance distribution. From the assignment of the radiance temperature with the FRs, the spectral irradiance of a set of FEL lamps is determined. The detector-based and the gold freezing blackbody-based spectral irradiances are compared, and the uncertainties of the detector-based spectral irradiance scale are discussed.

2. Experimental Approach

A. Radiance Temperature Determinations with Filter Radiometers

A schematic of the measurements is shown in Fig. 2. Both the spectroradiometer and the FRs reside on a common moving optical table. The FRs are first used to determine the radiance temperature of the HTBB; and thus with knowledge of the radiance temperature, the spectral irradiance responsivity of the spectroradiometer is assigned by use of a precision aperture on the integrating-sphere receiver (ISR) with the knowledge of the distance between the ISR and the precision aperture in front of the blackbody. The spectral irradiance of the 1000-W quartz tungsten–halogen lamp (type FEL) is then assigned by use of the spectral irradiance responsivity of the spectroradiometer.

The FRs are constructed with broadband filters and silicon detectors that are both temperature stabilized as shown in Fig. 3. A precision aperture is placed in front of the filter–detector package, and the aperture area is measured separately in the NIST High-Accuracy Aperture Measurement Facility to a relative combined expanded ($k = 2$) uncertainty of 0.01%.[11] The precision apertures attached to the FRs range from 4.0 to 4.4 mm in diameter. The detectors are calibrated for absolute spectral power responsivity on the NIST Spectral Comparator Fa-

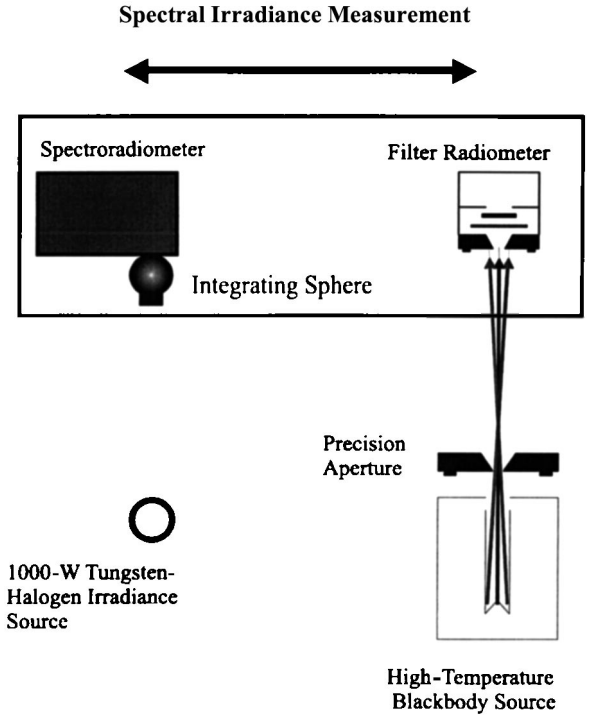

Fig. 2. Schematic of the laboratory setup used for the spectral irradiance scale realization showing the positions of the HTBB, the FRs, the spectroradiometer, and the FEL lamp.

cility (SCF),[12] and the power responsivity is converted to spectral irradiance responsivity from knowledge of the aperture area. A total of three detectors are used, and the absolute spectral power responsivities are shown in Fig. 4. Both filter radiometers FR2 and FR4 have photopic response filters resulting in a broad spectral responsivity. The FR3 has greater spectral responsivity to shorter wavelengths then the other two radiometers, with a drop in responsivity near 400 nm. The broadband radiometers were chosen for increased long-term stability, as compared with narrowband interference filters.[13]

The radiance temperature of the HTBB is found with a measurement equation, which describes the optical flux transfer with circular and coaxial source

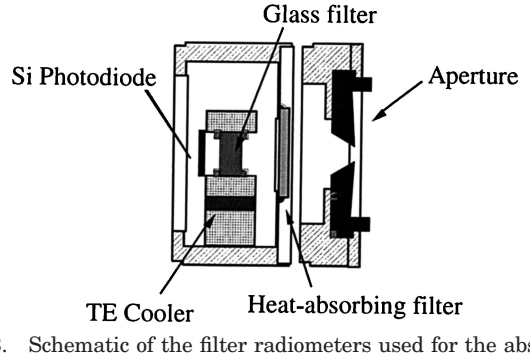

Fig. 3. Schematic of the filter radiometers used for the absolute temperature determination of the HTBB.

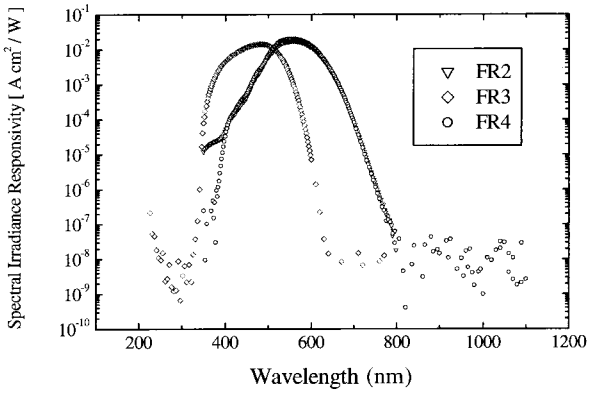

Fig. 4. Absolute spectral irradiance responsivities of the FRs used in the scale realization. Both filter radiometers FR2 and FR4 are constructed with broadband photopic response filters that differ in responsivity only slightly below 400 nm.

and receiver apertures.[14] For a FR, the signal s is given by

$$S = \frac{G\pi {r_{\mathrm{BB}}}^2 \pi r^2 (1 + \delta)}{D^2} \epsilon \int R(\lambda) L(\lambda, T) d\lambda, \quad (1)$$

where ϵ is the emissivity and R is the absolute spectral power responsivity. The geometric factors D and δ are given by $D^2 = d^2 + r^2 + {r_{\mathrm{BB}}}^2$ and $\delta = r^2 {r_{\mathrm{BB}}}^2 / D^4$, where r_{BB} and r are the radius of the blackbody aperture and the FR apertures, respectively, and d is the distance between the FR aperture and the blackbody aperture. G is the preamplifier gain and L is the spectral radiance found by use of the Planck radiation law. The radiance temperatures are found when we iteratively change the blackbody temperature in Eq. (1) until an exact match of the calculated signal to the measured signal is found.

The uncertainties of the radiance temperatures found with the FRs are primarily determined by the uncertainties in the spectral power responsivity. Figure 5(a) plots the expanded uncertainties of the SCF in the spectral power responsivity measurements. The lowest uncertainties are maintained in the visible wavelength region from 400 to 900 nm where the spectral power responsivity of the Si-trap transfer detector can be smoothly interpolated between the discrete laser calibration wavelengths of the HACR. The uncertainties of the spectral power responsivity can be converted directly to uncertainties in temperature by use of the derivative of the Wien approximation with respect to temperature:

$$\frac{\Delta L}{L} = \frac{c_2}{\lambda} \frac{\Delta T}{T^2} \quad (2)$$

is the relationship between the uncertainty in radiance L and the uncertainty in blackbody temperature T; c_2 is the second Planck's constant, 1.4387752 cm/K; and λ is the wavelength. The Wien approximation is used to simplify the handling of equations. Under these experimental conditions, no appreciable

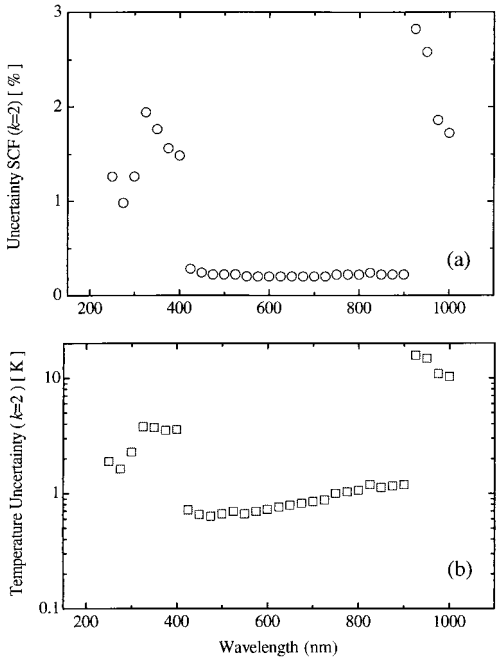

Fig. 5. (a) Expanded uncertainties of the NIST SCF for spectral power responsivity showing the low expanded uncertainties (0.22%) between 400 and 900 nm. (b) The uncertainties in the spectral power responsivity converted to temperature uncertainties by use of the derivative of the Wien approximation at 3000 K.

differences exist between Eq. (2) and the similar differential equation found when we use Planck's radiance law in the wavelength between 250 and 2400 nm. Because of the changes in the shape of the blackbody radiance with temperature as described in the Planck radiance law, the temperature uncertainties are both dependent on temperature as well as wavelength. The corresponding uncertainties in radiance temperatures are plotted in Fig. 5(b) for a blackbody temperature of 3000 K, where the lowest temperature uncertainties exist in the spectral region between 400 to 900 nm.

B. Description of the Facility for Automated Spectroradiometric Calibrations

All the experimental research described in this paper was performed in the Facility for Automated Spectroradiometric Calibrations (FASCAL), with the exception of the spectral power responsivity measurements of the FRs.[6] Briefly, the detector system consists of a prism-grating double monochromator with custom-modified entrance and exit optics. A simplified schematic of FASCAL is shown in Fig. 2. The light is collected with an off-axis spherical mirror with either an integrating receiver for spectral irradiance or a flat plane mirror for spectral radiance. The measurements from 250 to 900 nm were performed with a photomultiplier tube in dc measurement mode. We performed the measurements from 800 to 2400 nm using an InGaAs detector in photovoltaic mode using a mechanical light chopper at 290 Hz with phase-sensitive detection. A significant improvement to the FASCAL detection system is due to the replacement of the PbS detector [$D^* = 4 \times 10^{11}$ (cm/Hz$^{1/2}$)/W] with the extended InGaAs detector [$D^* = 2 \times 10^{12}$ (cm/Hz$^{1/2}$)/W], resulting in a standard deviation of signals $<0.05\%$ when a 1000-W FEL lamp is measured from 800 to 2300 nm. The spectrometer and the detector enclosure are also continuously purged with air filtered to remove CO_2 and H_2O, thus improving the long-term stability of the detector system.

C. Description of the High-Temperature Blackbody

One of the technological advances that makes possible the realization of the detector-based spectral irradiance scale is the development of pyrolytic graphite blackbodies, enabling extended operations near 3000 K without rapid degradation of the cavity. The HTBB used in this study consists of pyrolytic graphite rings with an inner diameter of 24 mm stacked to form a cavity with a depth of 14.5 cm. The cavity bottom consists of an inverted cone with an apex angle of approximately 150°, and the radiance at the backside of the cavity bottom is imaged through an opening at the rear of the cavity by use of a fused-silica lens onto a temperature-stabilized photometer for operation in closed-loop configuration. The lens also serves to seal the rear of the blackbody cavity to atmosphere. The current of the HTBB power supply is adjusted with a control loop to maintain a constant output from the photometer. Although the spectral irradiance in the ultraviolet wavelength region could be increased with higher temperatures, the HTBB was operated near 2950 K to avoid possible changes in the spectral emissivity of the blackbody that are due to the sublimation of the graphite.[15] Because the graphite rings expand approximately 10% from room temperature to near 3000 K, the current was increased at 0.1 A/s to nearly 510 A at 2950 K to allow gradual expansion of the cavity. The HTBB was also turned off in a similar manner to avoid thermophysical shocks.

Figure 6 is a plot of the radiance temperatures measured during a single day of measurements from 9:30 to 14:00 with FR2, FR3, and FR4. The feedback detector is a temperature-stabilized Si photodiode with a photopic response filter. The optical feedback is found to stabilize the HTBB to ± 0.0004 V at a full signal of 4.4 V. Figure 6 shows that the HTBB temperature was stable to <0.5 K over the duration of the 5-h measurement. The expanded uncertainties of the temperatures are shown for the FR2 temperatures that overlap the temperatures measured with FR3 and FR4. The three FRs agree in radiance temperature determinations to <0.5 K, in agreement with the combined expanded uncertainty in temperature of 0.86 K at 2950 K.

Each of the FR measurements is an independent determination of temperature when a primary thermometer is used. A primary thermometer is distinguished from a secondary thermometer in that the temperature is obtained by use of a primary thermometer without use of any adjustable parameters.[16]

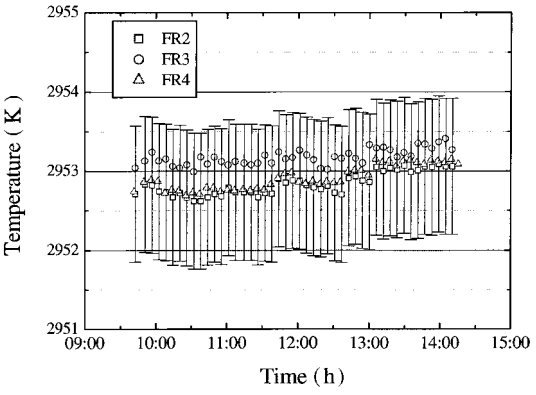

Fig. 6. Temporal stability measurement of radiance temperatures with the FRs. The expanded uncertainties in temperature of ±0.86 K are shown for FR2. The temporal drift in the HTBB temperature is less than 0.5 K over the duration of the nearly 5-h monitoring time.

The temperature of the HTBB increased at most by 1 K over 20 h of continuous operation with constant optical feedback control by use of the optical output from the rear of the cavity. The slight increase in temperature over time is possibly attributable to the opening at the rear of the cavity that gets smaller from carbon deposits at the edges of the opening. The HTBB was operated with an open cavity with continuous 0.5-1/min purge of argon from the rear of the housing and the argon exiting through the front opening of the cavity.

D. Verification of the High-Temperature Blackbody as a Planckian Radiator

To determine the spectral emissivity of the HTBB, the spectral radiance of the HTBB was measured from 250 to 2400 nm at discrete wavelengths by comparison with a VTBB with a high emissivity. Any temperature nonuniformity of the cavity would lead to deviations of the HTBB spectral radiance from a single-temperature Planck radiance. For these comparisons, the temperature of the VTBB was set at 2687 K, and the temperature of the HTBB was set at 2950 K. Although the temperatures are different, the radiance ratios did not differ even at 250 nm, where the differences are greatest, by more than a factor of 7. Furthermore, prior to these measurements, the linearity of the spectroradiometer was measured at various wavelengths with the portable Beamconjoiner[17] and was found to be linear under these experimental conditions. The spectral radiance determinations were performed before and after spectral irradiance transfer to a set of 1000-W FEL lamps. The checks of the HTBB as a Planckian radiator were performed to verify that the HTBB did not change in the spectral distribution because the FRs are used to measure over a relatively broad spectral region.

The spectral radiance measurements of the HTBB were performed with the aperture in front of the spherical input mirror with the spectroradiometer reduced to 4 cm in diameter, resulting in $F/25$ focused at the opening of the HTBB at the plane of the water-cooled aperture. The reduction in the opening of the spherical input mirror resulted in a circular target of 12 mm in diameter at the bottom of the HTBB cavity. To keep the same target area constant for the measurements, in both the spectral irradiance and the spectral radiance modes, the HTBB was mounted on a motorized translation stage for control of the distance between the HTBB and the measuring instruments. If possible, the same area at the rear of the HTBB should be viewed for all measurements to avoid errors from the possible spatial nonuniformity of the HTBB.

We determined the temperature of the VTBB using spectral radiance ratios at 655 nm to a vacuum tungsten-filament lamp maintained at the freezing temperature of gold as prescribed in the ITS-90. The spectral radiance of the HTBB was determined at discrete wavelengths by comparison with the VTBB and also determined from the radiance temperature found with the FRs. The radiance temperatures of the HTBB found with the FRs were in agreement with those found with the ITS-90 ratios to within 0.5 K in all cases in which such comparisons were performed. We compared the respective blackbodies using spectral radiance ratios:

$$L_{\lambda,\mathrm{HTBB}} = L_{\lambda,\mathrm{VTBB}} f_\lambda \frac{S_{\lambda,\mathrm{HTBB}}}{S_{\lambda,\mathrm{VTBB}}}. \tag{3}$$

The L_λ and the S_λ denote the spectral radiance and the measured spectral radiance response of the HTBB and the VTBB, and f_λ is the possible linearity correction to the response ratios. The spectral radiances of the HTBB were found to conform to a single-temperature Planck radiance law to within the combined uncertainties of the measurements as shown in Fig. 7. Figure 7 shows the percent differences from a single-temperature Planck radiance law with the temperature of the HTBB determined with the FRs and the spectral radiances determined with the VTBB. The errors bars on the individual comparisons correspond to the expanded uncertainty of 0.86 K at 2943.4 K converted to a spectral radiance uncertainty by use of the derivative of the Wien approximation from Eq. (2). As expected for comparison of two blackbodies, the differences in the spectral radiance become smaller with increasing wavelength, but there are no discernible increasing spectral differences toward the shorter wavelengths, as would be expected if either of the temperature assignments of the respective blackbodies were in error. The differences between the detector-based radiance temperatures and the source-based determinations also agree with the previous measurements, which also showed differences of $<0.5\%$ from 250 to 1000 nm.[18]

E. Spectral Irradiance Transfer to 1000-W FEL Lamps

The spectral irradiance assignment of twelve 1000-W FEL working standard lamps occurred over a two-

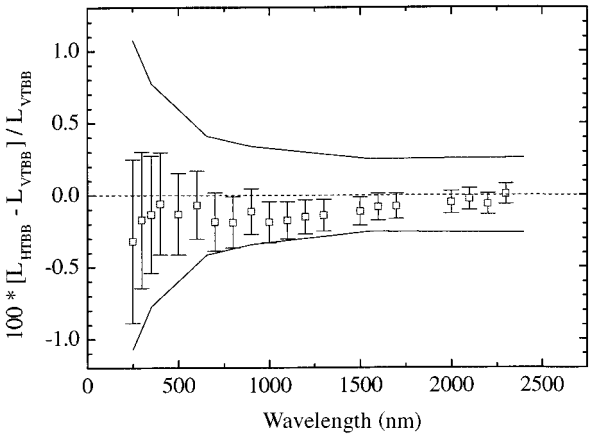

Fig. 7. Spectral radiance differences of the HTBB from a single-temperature Planck radiance as assigned by use of the FRs to the spectral radiances assigned by use of the VTBB. The error bars indicate the 0.86 K expanded temperature uncertainty at 2950 K converted to spectral radiance uncertainties, and the continuous curves indicate the expanded uncertainties of the spectral radiance scale.

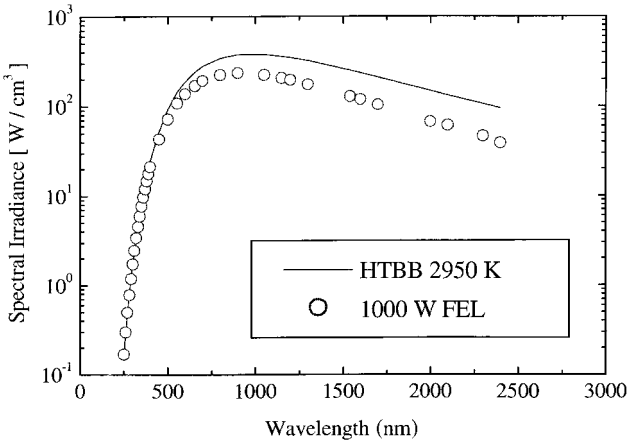

Fig. 8. Spectral irradiance of the HTBB at 2950 K with the measurement parameters as described with the spectral irradiances of a typical 1000-W FEL lamp. The measurement parameters were chosen to closely match the signals of both sources.

week period from 28 September to 12 October 2000. The spectral irradiances of a group of three lamps were assigned at one time, and the measurements were separated into the ultraviolet and the visible wavelength region (250–900 nm), and the shortwave infrared region (800–2400 nm). Because there are four separate FEL lamp measurement stations, each of the measurements of individual lamps was performed in a different station by use of different shunt resistors, power supplies, and lamp mounts. Each of the lamp stations was checked for possible position effects, and no perceptible effects from station-to-station variations were found.

The HTBB was turned on at least 2 h before use and was temperature-stabilized by the optical feedback. The temperature of the HTBB was assigned by use of the FRs, and the spectral irradiance responsivity of the spectroradiometer was assigned by use of the known spectral irradiance of the HTBB. All the spectral irradiance responsivity transfers to the spectroradiometer were done at a distance of 43.406 cm ($\pm$0.005 cm) from the HTBB aperture to the 1-cm^2-area aperture of the ISR, resulting in a 24.7-mm-diameter circular target area at the cavity bottom. The spectral irradiance responsivity of the spectroradiometer is assigned by use of the known spectral irradiance of the HTBB at the input aperture of the ISR:

$$E_{\lambda,\mathrm{HTBB}} = \frac{L(\lambda, T)\pi r_{\mathrm{BB}}{}^2}{D^2}, \tag{4}$$

with the measurement parameters as defined in Eq. (1).

After the spectral irradiance responsivity assignment of the spectroradiometer, the spectral irradiance of a group of three FEL lamps was assigned with each lamp measured in three separate source positions. The spectral irradiance of each lamp was assigned by

$$E_{\lambda,\mathrm{FEL}} = E_{\lambda,\mathrm{HTBB}} f_\lambda \frac{S_{\lambda,\mathrm{FEL}}}{S_{\lambda,\mathrm{HTBB}}}, \tag{5}$$

where $E_{\lambda,\mathrm{FEL(HTBB)}}$ is the spectral irradiance of the FEL lamp (HTBB), $S_{\lambda,\mathrm{FEL(HTBB)}}$ is the net signal from the FEL lamp (HTBB) measured with the spectroradiometer, and f_λ is the linearity correction factor for the comparison. With use of a shutter, the background signals were subtracted from the total signals to obtain the net signals. The distance of the HTBB from the ISR was also chosen such that the same gain factors could be used to measure both the FEL and the HTBB. Figure 8 is a plot of the calculated spectral irradiances of the 1000-W FEL along with the HTBB at 2950 K with the limiting aperture of 9.9933 mm ($\pm$0.0002 mm) in diameter and the ISR aperture of 11.2838 mm ($\pm$0.0002 mm) in diameter separated by a distance of 43.406 cm ($\pm$0.005 cm). At all wavelengths, Fig. 8 shows that the HTBB has a greater spectral irradiance than the FEL lamp. Although the spectral irradiance changes by a factor $>10^3$ from 250 to 2400 nm, the HTBB/FEL signal ratio does not exceed 2.5. The close match of the irradiances was chosen to minimize possible errors resulting from signal-to-noise ratio, nonlinearity, and stray-light effects.

3. Uncertainty Analysis of the Detector-Based Spectral Irradiance Scale

The discussion of the uncertainties associated with the detector-based spectral irradiance scale realization is separated into parts. Because the absolute radiance temperature determination of the HTBB is performed with FRs with peak spectral responsivities near 550 nm, the expanded uncertainties in the spectral irradiance measurement at 550 nm is discussed first. The spectral irradiance uncertainties are converted into temperature uncertainties by use of the

Table 1. Expanded Component Uncertainties in the Spectral Irradiance Measurement with the FR at 550 nm

Source of Uncertainty (550 nm)	Fractional Uncertainty	Expanded Uncertainty (%)
Spectral power responsivity, FR	$\frac{\Delta R}{R}$	0.22
Solid-angle factor, HTBB/FR		0.026
Area of detector aperture	$\frac{\Delta A}{A}$	0.02
Area of HTBB aperture	$\frac{\Delta A}{A}$	0.02
Measurement precision, HTBB/FR		0.006
Amplifier gain	$\frac{\Delta G}{G}$	0.006
Combined expanded uncertainty ($k = 2$)		0.26

derivative of the Wien approximation. The Wien approximation is used because the measurements are performed at short wavelengths from the peak wavelength of the 3000 K Planck spectral radiance. The uncertainties of the spectral irradiances of the primary working standards are assigned. Finally, the expanded uncertainties of the issued standards are assigned with additional uncertainty added to account for the temporal changes of the working standard lamps.

The uncertainties associated with the detector-based temperature determinations of the HTBB can be found from the uncertainty analysis of Eq. (1) as shown in Table 1. The individual components are listed in descending order of importance, with the uncertainty that is due to the spectral power responsivity dominating. Additional sources of uncertainty from the alignment and aperture area measurements are small. The expanded spectral irradiance responsivity uncertainty at 550 nm of 0.26% leads to an expanded temperature uncertainty of 0.86 K at 2950 K.

Table 2 describes the additional uncertainties associated with the HTBB spectral irradiance including the components that are due to spectral emissivity, spatial uniformity, and temporal stability. The first row shows the expanded uncertainty of the spectral irradiance that is due to the 0.86 K expanded temperature uncertainty at 2950 K. The uncertainties that are due to the spectral emissivity and the spatial uniformity of the HTBB are then assigned. The temporal stability of the HTBB was measured and also constantly monitored by use of the optical feedback at the rear of the cavity. The uncertainties in the alignment of the apertures and in the distance measurements are included in the geometric factor uncertainty.

The detectors used in the spectroradiometers have shown better than 0.1% ($k = 2$) stability during the spectral irradiance measurements. However, the increase of the uncertainty at 2400 nm because the stability of the spectroradiometer responsivity is due to the performance of the InGaAs detector. A substantial contribution to the total uncertainty comes

Table 2. Expanded Uncertainties of the Detector-Based 2000 Spectral Irradiance Scales of the Primary Working Standards and the Issued Standards[a]

	Wavelength (nm)							
Component	250	350	655	900	1600	2000	2300	2400
HTBB temperature uncertainty (0.86 K at 2950 K)	0.57	0.41	0.22	0.16	0.09	0.08	0.07	0.07
HTBB spectral emissivity	0.1	0.1	0.1	0.1	0.1	0.1	0.1	0.1
HTBB spatial uniformity	0.1	0.1	0.1	0.1	0.1	0.1	0.1	0.1
HTBB temporal stability (0.1 K/h)	0.07	0.05	0.03	0.02	0.01	0.01	0.01	0.01
Geometric factors in irradiance transfer	0.1	0.1	0.1	0.1	0.1	0.1	0.1	0.1
Spectroradiometer responsivity stability	0.1	0.1	0.1	0.1	0.1	0.1	0.1	0.5
Wavelength accuracy (0.1 nm)	0.58	0.38	0.18	0.005	0.011	0.013	0.011	0.011
Lamp/spectroradiometer transfer	0.1	0.1	0.1	0.1	0.1	0.1	0.1	0.1
Lamp current stability	0.08	0.06	0.03	0.02	0.02	0.01	0.01	0.01
Uncertainty of the primary working standards, total ($k = 2$)	0.85	0.60	0.36	0.28	0.24	0.24	0.23	0.54
Lamp-to-lamp transfer	0.1	0.1	0.1	0.1	0.1	0.1	0.1	0.1
Long-term stability of working standards	1.31	0.94	0.50	0.36	0.20	0.16	0.14	0.14
Uncertainty of the issued standards, total ($k = 2$)	1.56	1.12	0.63	0.47	0.33	0.31	0.29	0.57

[a]Uncertainty ($k = 2$) (%).

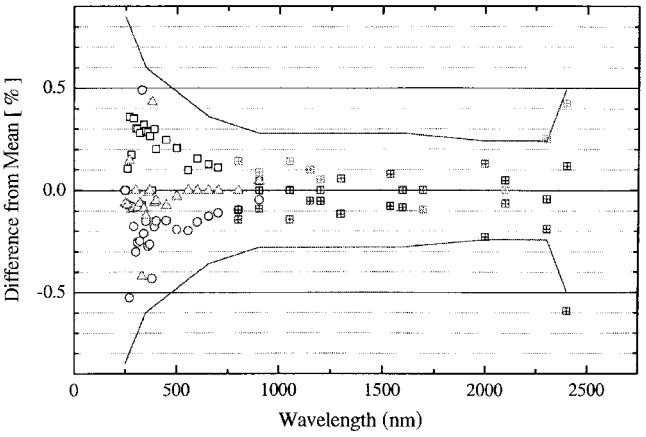

Fig. 9. Percent differences from the mean of three separate spectral irradiance scale realizations performed on four separate days. The differences are shown with the assigned expanded uncertainties of the working standards for the detector-based spectral irradiance scale.

from the uncertainty in the absolute wavelength. The wavelength drive of the prism-grating spectroradiometer has an absolute optical encoder attached to the shaft, and piecewise continuous polynomial corrections are applied to achieve ±0.05-nm standard uncertainty in the wavelength. For determination of the uncertainties on the issued standards, additional components arising from the lamp-to-lamp transfer and long-term stability of the working standards are added. A substantial increase in the total uncertainties arises from the possible temporal drift of the working standards. All lamp standards are subjected to a screening procedure for temporal drift, and lamps that change by more than 0.5% at 650 nm over the duration of 24 operational hours are rejected from further evaluation as possible standards.[6] The temporal drift is found to be inversely proportional to the wavelength and is accordingly larger at the shorter wavelengths.

To determine whether the uncertainties were correctly estimated, data from separate independent scale realizations of a FEL lamp (F210) were analyzed. Figure 9 shows the percent differences from the mean in the detector-based spectral irradiance of the lamp with three independent assignments from 250 to 900 nm and from three other separate assignments from 800 to 2400 nm over four separate days. The spectral irradiance assignments show that the three independent scale realizations for a particular wavelength region are all within the assigned ($k = 2$) expanded uncertainties of the 2000 spectral irradiance scale. The temperature of the HTBB was determined on each of the days during the realization, and the spectral irradiance responsivity was assigned approximately 30 min after a temperature assignment by use of the FRs. The separate spectral irradiance assignments are all within the expanded uncertainties. The slight upturn in the uncertainties at 2400 nm is due to the rapidly decreasing spectral responsivity of the InGaAs detector near the bandgap energy of the material. The spectral shape of the expanded uncertainty follows the inverse wavelength dependence expected for a scale based on a temperature determination of a HTBB.

Table 3. Comparison of the Expanded Uncertainties in the Spectral Irradiance Scales of the 1990 and 2000 Scale Realizations

Wavelength (nm)	Expanded Uncertainties in Spectral Irradiance (%) ($k = 2$)	
	1990	2000
250	1.8	1.56
350	1.1	1.12
655	0.9	0.63
900	1.1	0.47
1600	1.4	0.33
2300	3.8	0.29
2400	4.4	0.57

4. Comparison of the Detector- and Source-Based Spectral Irradiance Scales

Table 3 shows the total expanded uncertainties of the spectral irradiance scales from the 1990 and the 2000 realizations. Figure 10 shows that the detector-based spectral irradiance scale results in the reduction in the uncertainties in the 250–900-nm wavelength regions by a factor of 2 and a greater reduction up to a factor of 10 in the uncertainties from the 900- to 2400-nm wavelength region. The reduction in the uncertainties is primarily due to the elimination of the ISS that was used as a transfer artifact to obtain spectral irradiance from the spectral radiance assignment. The spectral irradiance of the ISS was lower than that of the 1000-W FEL and was especially difficult to measure in the infrared wavelength region with the previous PbS detector, resulting in the large uncertainties. The detector-based spectral irradiance utilizes the HTBB, which has greater spectral irradiance than the 1000-W FEL lamp at all wavelengths, and the improved InGaAs detector in the infrared further reduces the measure-

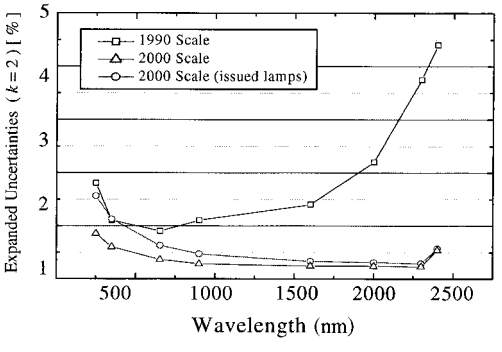

Fig. 10. Comparison of the expanded uncertainties of the 1990 scale realization along with the expanded uncertainties of the 2000 scale realization. The expanded uncertainties of the issued lamps are greater because of the additional component of the long-term temporal stability of the working standards.

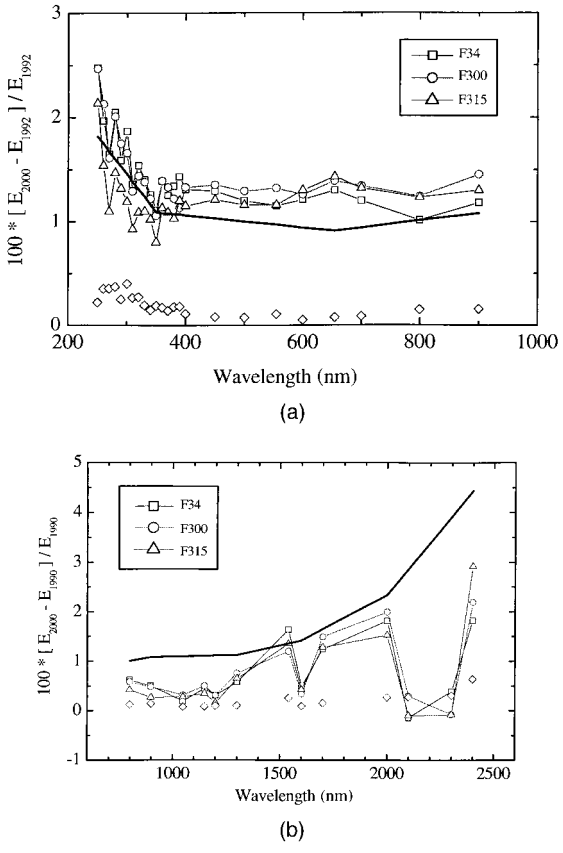

Fig. 11. (a) Comparison from 250 to 900 nm of the spectral irradiance assigned to the check standard lamps in 1992 with the detector-based spectral irradiance assignments. The expanded uncertainties assigned in 1990 are shown as the dark curve. The standard deviations of the mean of the three lamps are shown as open diamonds, indicating the good agreement between the three lamps. (b) A comparison from 800 to 2400 nm of the three check standard lamps of the 1990 spectral irradiance assignment with the detector-based spectral irradiance assignment. The standard deviations of the mean of the three lamps are shown as open diamonds along with the expanded uncertainties of the 1990 scale shown by the dark curve.

ment uncertainties. The spectral shape of the uncertainties also has the characteristic $1/\lambda$ dependence of the decrease in uncertainties with increasing wavelength that can be seen in Eq. (2).

The differences in the spectral irradiance between the source-based and the detector-based spectral irradiance scale are shown in Fig. 11(a) for a set of check standard lamps (F34, F300, F315) in the wavelength region from 250 to 900 nm and in the wavelength region from 800 to 2400 nm in Fig. 11(b). At NIST, a set of lamps (working standard lamps) are used for routine calibrations, and another set of lamps (check standard lamps) are set aside to verify that the working standard lamps did not drift. The check standards were used approximately twice a year to verify that the working standard lamps did not changed; thus the total operational hours on the check standards are typically much less than the operational hours of the working standards.

In Fig. 11(a) the comparison of the detector-based scale with the source-based scale shows that the difference of the NIST spectral irradiance assignments is greater than their assigned expanded uncertainties by $\leq 0.5\%$. The sawtooth oscillations that can be seen in the source-based spectral irradiance evident at <400 nm is correlated in all the lamps and is evident to a lesser extent at longer wavelengths. The correlated oscillations are attributed to the experimental procedure used in the previous spectral irradiance scale realization of 1992. In the realization of 1992, the ISS was assigned a spectral radiance at a particular wavelength, and the spectral irradiance of a set of three lamps was assigned immediately by use of the spectral irradiance of the ISS. Thus the spectral irradiance at each wavelength is realized separately and independently; and especially in the ultraviolet region, the oscillations could arise from a possible temporal drift of the ISS. Our ability to maintain the spectral irradiance over ten years using a set of stable lamps is shown by the agreement among lamps F34, F300, and F315 as compared with the detector-based spectral irradiance scale. The standard deviation of the mean found when we used the percent differences of the three lamps from the detector-based scale is plotted in Fig. 11(a) with the open diamonds and shows that the lamps have stayed together as a group to $<0.5\%$ from 1992.

In the shortwave infrared wavelength region, the source-based spectral irradiance scale from 800 to 2400 nm was last realized from the gold freezing-point blackbody in 1990. A new spectral irradiance scale realization was attempted in 1992 from 250 to 2400 nm with a more stable ISS, but the scale realization in the infrared region was not completed because of the insufficient spectral irradiance of the 1992 ISS in the infrared and the low signal-to-noise ratio from the PbS detector. The discontinuity at 800 and 900 nm for a common lamp is due to the separate scale realizations performed in 1990 and in 1992. For assignment of spectral irradiance of the issued lamps, the different spectral irradiance values were averaged to obtain a single value at those wavelengths. As in the comparisons from 250 to 900 nm, the check standard lamps remained close together as a group with their spectral irradiances much better than $<0.5\%$ as shown in Fig. 11(b) by the open diamonds at the bottom of the figure. Two noticeable drops in the irradiances are observed at 1600 and 2100 nm in the comparison of the scales. The Consultative Committee on Photometry and Radiometry (CCPR) comparison of 1990[19] also showed that the 1% drop at 1600 nm and the nearly 2% drop at 2100 nm were seen in all comparisons with the other countries, indicating that the two spectral features were inherent to the NIST spectral irradiance scale of 1990. The differences of the detector-based spectral irradiance scale to the source-based scale of 1990 show that the assignment of the spectral irradiances were within their stated uncertainties since 1990.

These comparisons to the check standards should reflect the differences between the new detector-based scale and the scale realized in 1992, and more

importantly, the scale realized in 1990 before and after the international comparison of spectral irradiance organized by the CCPR. If the differences seen can be extrapolated to the CCPR comparisons in 1990, then the NIST spectral irradiance scale for the comparison would have been approximately 1% low in the visible and approximately 2% low in the ultraviolet wavelength region. The large variations in the spectral irradiance scales of the individual countries preclude discerning whether the differences found between the detector-based scale and the 1990 scale could be detected in the international intercomparison.

5. Discussion

Because of the long history of the spectral irradiance scale at NIST and the resulting wide usage of the FEL lamps issued by NIST, the one most important result is the relationship between the spectral irradiances from the detector-based scale realization of 2000 and the previously assigned spectral irradiances. Figures 12(a) and 12(b) show the means of the spectral irradiances of the three working standards used to assign FEL lamps to the detector-based spectral irradiance scale along with the expanded uncertainties of the 1992 scale realization. In the wavelength region from 250 to 900 nm, only one point, at 250 nm, falls beyond the 0.5% of the expanded ($k = 2$) uncertainties; and if the uncertainties are increased to 3σ ($k = 3$), then all the values are within uncertainties. In the infrared region from 900 to 2400 nm, only three values exceed the expanded uncertainties by more than 0.5%, and again all the differences fall within the 3σ ($k = 3$) uncertainties.

Because we have shown that the radiance temperature scale and the spectral radiance scale at NIST are both in agreement with the detector-based scales within the combined uncertainties, what are the reasons for the observed discrepancies in the spectral irradiance scales? In the infrared wavelength region from 900 to 2400 nm, the spectral irradiances of the check standard lamps are within the assigned expanded uncertainties, although the irradiances were assigned in 1990. The larger deviations of the working standards can be attributed to the longer operational hours and reveal that the spectral irradiances of the working standards should have been verified against the check standards at shorter time intervals.

Some of the differences from 250 to 900 nm that can be seen in Fig. 12(a) can also be attributed to temporal drift of the working standards because of longer operational hours, but the comparison with the check standards shows that much of the differences between the detector-based scale and the scale realized in 1992 are also apparent in lamps that have not been utilized extensively. The spectral irradiance scales of 1990 and 1992 are both dependent on the radiance temperature and the spectral radiance scales. Because both the radiance temperature scales and the spectral radiance scales were found to

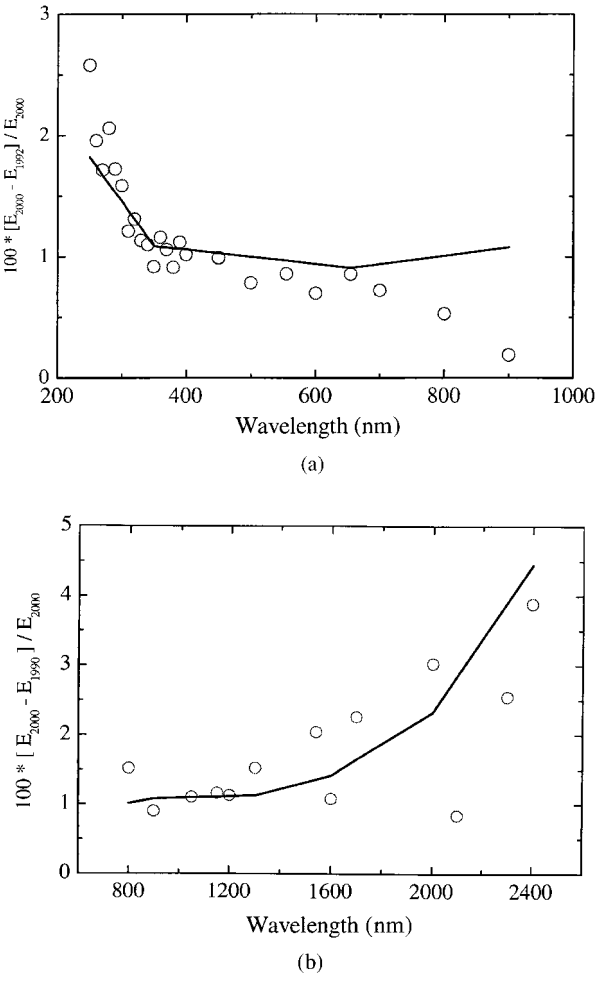

Fig. 12. (a) Comparison from 250 to 900 nm of the difference of the average of the spectral irradiances assigned in 1992 of three working standards F234, F302, and F210 to the detector-based spectral irradiances. The curve indicates the expanded uncertainties of the 1992 spectral irradiance scale. (b) A comparison from 800 to 2400 nm of the working standard lamps of the differences of the 1990 spectral irradiance scale to the detector-based scale. The curve indicates the expanded uncertainties of the 1990 spectral irradiance assignments.

be in agreement with the detector-based scale within the combined uncertainties, possible differences between the source-based and the detector-based spectral irradiances scales could have arisen in the process of deriving the spectral irradiance scale from the spectral radiance scale.

The long time period between the spectral irradiance scale realizations of 1992 and 2000 partly results from the experimental difficulties in the realizations of a spectral irradiance scale with the gold freezing-point blackbody. The need for numerous transfer artifacts and systematic corrections that are due to the less than optimal performance of these artifacts prohibited frequent scale realizations. The new detector-based spectral irradiance scale realization relies only on an accurate radiance temperature determination of a HTBB whose adherence to the Planck radiance law

was verified by comparison with a blackbody with a known high emissivity. Initially, the detector-based spectral irradiance scale realizations will be performed on an annual basis in FASCAL. With sufficient evidence that the spectral irradiance scale can be maintained on working standard lamps without increases in the errors that are due to long-term drift, the scale realizations will be performed on a less frequent basis.

In the past scale realizations, spectral irradiance assignments at additional wavelengths have been difficult because of the lengthy procedure needed for the realizations. The temporal drift of the transfer artifacts used in the realization resulted in the limited number of wavelengths of the spectral irradiance assignments of the working standards. Because the HTBB used in the detector-based spectral irradiance scale is temporally stable with a drift of <1 K in 20 h at 3000 K, spectral irradiance assignments of working standards are possible at many additional wavelengths if desired by the optical measurement community. These spectral irradiance calibrations at much finer wavelength intervals can help to resolve issues such as the optimal interpolation algorithm for use in the calibration of spectroradiometers.[20]

6. Effect of the Changes That Are Due to the Detector-Based Spectral Irradiance Scale

The greatest changes of the detector-based spectral irradiance scale realization result from the lower uncertainties, enabling measurements to be made with higher accuracy and confidence. However, if the dominant sources of the total measurement uncertainties were not due to the intrinsic scale uncertainties of the transfer artifact, then it would be difficult to utilize the lower uncertainties achieved with the detector-based scale. In addition, the small differences between the detector-based and the source-based spectral irradiance scales are within the expanded uncertainties of many measurement systems, including the spectroradiometers used in the ultraviolet monitoring of terrestrial solar spectral irradiance.[21]

In the photometric community, possible changes could arise in the calibration of sources for color temperature.[22] At NIST, color temperatures are assigned in the Photometric Calibration Facility by use of the relative spectral irradiance of FEL lamps. Because the spectral shapes of the source-based and the detector-based spectral irradiances in the wavelength region from 350 to 700 nm differ at most by $<0.5\%$ [Fig. 12(a)], the changes to the color temperature assignments will be negligible.

7. Conclusion

The realization of the NIST detector-based spectral irradiance scale was described. The realization is based on the absolute detector-based radiance temperature determinations of a HTBB and is now traceable to the HACR instead of a fixed-point blackbody. The differences in the spectral irradiances between the gold-point blackbody-based and the detector-based scales are discussed, and the differences are found to agree within the combined uncertainties of the measurements. The detector-based scale results in the reduction of the uncertainties from 250 to 2400 nm with the greatest reduction occurring in the spectral range from 1000 to 2400 nm with reductions by almost a factor of 10. The new detector-based spectral irradiance scale realization also corrects the correlated deviations from a smooth Planck radiance law that existed in the old spectral irradiance scale. Finally, the differences in the way that the scale is derived represent a fundamental change in the scale realization of spectroradiometric sources, and these results are only the beginning of the implementation of the detector-based source scales at NIST.

The authors gratefully acknowledge the help and encouragement of B. Carol Johnson, Robert Saunders, and Al Parr of the Optical Technology Division at all stages of this project. The authors also acknowledge the assistance of Tom Larason and George Eppeldauer in the development and characterization of the filter radiometers used in the scale realization.

References

1. A. C. Parr, "A national measurement system for radiometry, photometry, and pyrometry based upon absolute detectors," NIST Tech. Note 1421 (National Institute of Standards and Technology, Gaithersburg, Md., 1996).
2. T. R. Gentile, J. M. Houston, and C. L. Cromer, "Realization of a scale of absolute spectral response using the National Institute of Standards and Technology high-accuracy cryogenic radiometer," Appl. Opt. **35,** 4392–4403 (1996).
3. C. L. Cromer, G. Eppeldauer, J. E. Hardis, T. C. Larason, and A. C. Parr, "National Institute of Standards and Technology detector-based photometric scale," Appl. Opt. **32,** 2936–2948 (1993).
4. Y. Ohno, "Improved photometric standards and calibration procedures at NIST," J. Res. Natl. Inst. Stand. Technol. **102**, 323–331 (1997).
5. K. D. Mielenz, R. D. Saunders, A. C. Parr, and J. J. Hsia, "The 1990 NIST scales of thermal radiometry," J. Res. Natl. Inst. Stand. Technol. **95,** 621–629 (1990).
6. J. H. Walker, R. D. Saunders, J. K. Jackson, and D. A. McSparron, "Spectral irradiance calibrations," NBS Measurement Services SP 250-20 (National Bureau of Standards, Gaithersburg, Md., 1987).
7. H. J. Kostkowski, D. E. Erminy, and A. T. Hattenburg, "High-accuracy spectral radiance calibration of tungten-strip lamps," Adv. Geophys. **14,** 111–127 (1970).
8. K. D. Mielenz, R. D. Saunders, and J. B. Shumaker, "Spectroradiometric determination of the freezing temperature of gold," J. Res. Natl. Inst. Stand. Technol. **95,** 49–67 (1990).
9. V. I. Sapritsky, "Black-body radiometry," Metrologia **32,** 411–427 (1995–1996).
10. H. Preston-Thomas, "The ITS-90," Metrologia **27,** 3–10 (1990).
11. J. B. Fowler, R. D. Saunders, and A. C. Parr, "Summary of the high-accuracy aperture-area measurement capabilities at the NIST," Metrologia **37,** 621–623 (2000).
12. T. C. Larason, S. S. Bruce, and A. C. Parr, "Spectroradiometric detector measurements: Part I—Ultraviolet detectors and Part II—Visible to near-infrared detectors," NIST Measurement Services SP 250-41 (National Institute of Standards and Technology, Gaithersburg, Md., 1998).

13. P. Sperfeld, J. Metzdorf, S. Gala Yousef, K. D. Stock, and W. Möller, "Improvement and extension of the blackbody-based spectral irradiance scale," Metrologia **35,** 267–271 (1998).
14. H. W. Yoon and C. E. Gibson, "Determination of radiance temperatures using detectors calibrated for absolute spectral power response," in *Proceedings of the Seventh International Symposium on Temperature and Thermal Measurements in Industry and Science*, J. Dubbeldam and M. J. de Groot, eds. (Edauw and Johannisen, The Netherlands, 1999), pp. 737–742.
15. P. Sperfeld, S. Galal-Yousef, J. Metzdorf, B. Nawo, and W. Moller, "The use of self-consistent calibrations to recover absorption bands in the black-body spectrum," Metrologia **37,** 373–376 (2000).
16. T. J. Quinn, *Temperature* (Academic, London, 1990).
17. A. Thompson and H. M. Chen, "Beamcon III: a linearity measurement instrument for optical detectors," J. Res. Natl. Inst. Stand. Technol. **99,** 751–755 (1994).
18. H. W. Yoon and C. E. Gibson, "Comparison of the absolute detector-based spectral radiance assignment with the current NIST-assigned spectral radiance of tungsten strip lamps," Metrologia **37,** 429–432 (2000).
19. J. H. Walker, R. D. Saunders, J. K. Jackson, and K. D. Mielenz, "Results of a CCPR intercomparison of spectral irradiance measurements by national laboratories," J. Res. Natl. Inst. Stand. Technol. **96,** 647–668 (1991).
20. L. K. Huang, R. P. Cebula, and E. Hilsenrath, "New procedure for interpolating NIST FEL lamp irradiances," Metrologia **35,** 381–386 (1998).
21. G. Bernhard and G. Seckmeyer, "Uncertainty of measurements of spectral solar UV irradiance," J. Geophys. Res. **104,** 14321–14345 (1999).
22. Y. Ohno, "Photometric calibrations," NIST Measurement Services SP 250-37 (National Institute of Standards and Technology, Gaithersburg, Md., 1997).